

Chapter 13

CORNEAL EFFECTS OF LASER RADIATION

RUSSELL L. McCALLY, PhD,* AND BRUCE E. STUCK, MS, ScD†

INTRODUCTION

- Anatomy of the Cornea
- Wavelength Dependence of Infrared Absorption
- Response Criteria
- Animal Models

CORNEAL INJURY THRESHOLDS AND PERMISSIBLE EXPOSURE LIMITS FOR CARBON DIOXIDE LASERS

- Epithelial Injury Thresholds
- Endothelial Injury Thresholds
- Corneal Stromal Effects

THERMAL MODELS AND TEMPERATURE MEASUREMENTS

CORNEAL EFFECTS AT OTHER LASER WAVELENGTHS

- Epithelial Injury Thresholds for Erbium Glass Laser Radiation
- Epithelial Injury Thresholds for Holmium Laser Radiation

SUMMARY

*Principal Staff Physicist (Retired), Johns Hopkins University Applied Physics Laboratory, Laurel, Maryland, and Johns Hopkins University Wilmer Eye Institute, 4940 Eastern Avenue, Baltimore, Maryland 21224

†Formerly, Detachment Director, US Army Medical Research Detachment—Walter Reed Army Institute of Research, 7965 Dave Erwin Drive, Brooks City-Base, Texas 78235

INTRODUCTION

Infrared radiation at wavelengths longer than 1.4 μm is absorbed to varying degrees by water in body tissue. Due to their relatively high water content and accessibility, the cornea and skin are particularly susceptible. Because corneal absorption of infrared radiation blocks retinal exposure, the infrared spectral region is typically regarded as "eyesafe"; however, this term is misleading. In fact, overexposure to infrared radiation can cause painful and visually disabling corneal injuries.

Anatomy of the Cornea

In addition to the tear layer, which is about 7 μm thick,¹ the human cornea is comprised of five distinct layers of tissue. From anterior to posterior, these are the epithelium, Bowman layer, stroma, Descemet membrane, and endothelium. The epithelium is about 50 μm thick and composed of several layers of cells. It is attached to a basement membrane that separates it from the Bowman layer. The Bowman layer is approximately 10 μm thick; it is acellular, composed of thin collagen fibrils aligned randomly in a ground substance. The stromal layer accounts for 90% of the human corneal

thickness, which averages 520 μm . The stroma is composed of layers of parallel collagen fibrils embedded in a ground substance. Interspersed between the collagen fibril layers are keratocytes; these cells account for 3% to 5% of the stromal volume. The Descemet membrane is a highly ordered network of very thin collagen filaments; in adults, this membrane is about 10 μm thick. The Descemet membrane is the basement membrane of the endothelium, which is a single cell layer about 3 μm thick. The endothelium actively pumps fluids into the anterior chamber to maintain corneal hydration at its normal physiologic value. Maintenance of proper hydration is essential for corneal transparency. Because human endothelium does not regenerate readily after injury, it is important that its health be maintained. The human cornea is 78% water by weight; the remaining 22% is composed of collagen, other proteins, glycosaminoglycans, and salts.²

Cells in all corneal layers are subject to thermal damage from absorbed infrared radiation. Further, temperatures above about 57 $^{\circ}\text{C}$ will cause the corneal collagen matrix to shrink.³ This effect is the basis for laser thermokeroplasty as a treatment for hyperopia.

Wavelength Dependence of Infrared Absorption

The absorption of radiation in a material is described by Beer's law, which is expressed as

$$(1) \quad I(z) = I_0 \exp(-\alpha z)$$

where $I(z)$ is the irradiance at a distance z into the material, I_0 is the incident irradiance, and α is the absorption coefficient. The value of the absorption coefficient depends upon material type and radiation wavelength. Figure 13-1 shows the absorption spectrum of water in the infrared range from 1.4 μm to 11 μm .⁴ Table 13-1 presents the values of α for water, physiological saline, and cornea at several infrared laser wavelengths of interest.⁴ Due to the thickness of the cornea (520 μm), its absorption spectrum cannot be measured for wavelengths greater than ~ 2.5 μm . Figure 13-2 shows plots of $I(z)/I_0$ as a function of distance into the cornea for laser wavelengths of 1.54 μm (erbium-doped [Er] fiber), 2.02 μm (thulium yttrium aluminum garnet [Tm:YAG]), and 10.6 μm (carbon dioxide [CO_2]). A schematic representation of the human cornea is also shown for reference. Note that CO_2 radiation is absorbed almost entirely in the epithelial layer, and Tm:YAG radiation is absorbed almost entirely in the cornea. By contrast, only $\sim 40\%$ of Er fiber laser radiation is absorbed in the entire depth of the cornea.

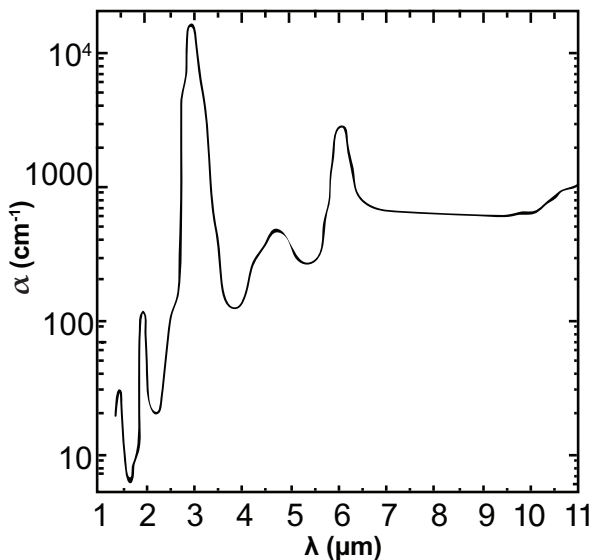


Figure 13-1. Absorption spectrum of water in the infrared range.

α : absorption coefficient; λ : wavelength

Data source: Maher EF. *Transmission and Absorption Coefficients for Ocular Media of the Rhesus Monkey*. Brooks Air Force Base, TX: US Air Force School of Aerospace Medicine; 1978. Report SAM-TR-78-32.

TABLE 13-1
ABSORPTION COEFFICIENTS FOR SEVERAL
INFRARED LASERS

Laser	Distilled Water α (cm ⁻¹)	Physiological Saline α (cm ⁻¹)	Cornea α (cm ⁻¹)
Er Fiber (1.54 μ m)	12.3	12.0	9.03
Tm:YAG (2.02 μ m)	55.0	57.5	38.1
Ho:YAG (2.10 μ m)	28.6	28.6	20.9
HF (2.7 μ m)	610	423	*
Er:YAG (2.94 μ m)	17,700	7,260	*
CO ₂ (10.6 μ m)	920	>2,000	*

*Due to the thickness of the cornea, its absorption spectrum cannot be measured for wavelengths greater than ~ 2.5 μ m.

α : absorption coefficient

CO₂: carbon dioxide

Er: erbium-doped

HF: hydrogen fluoride

Ho: holmium

Tm: thulium

YAG: yttrium aluminum garnet

Response Criteria

Once absorbed, infrared energy is rapidly converted to heat. This raises the temperature of the absorption volume. Heat is then conducted to deeper layers, whereupon temperature rises throughout the exposed tissue. Increased temperature is thus the combined result of direct radiation and heat conduction. Sufficiently high temperatures will cause thermal damage to exposed tissue. At very high irradiance or radiant exposure levels, this damage can be severe and may even cause tissue charring or ablation.⁵⁻⁸ This chapter, however, is primarily concerned with threshold damage.

In general, threshold injury involves only the corneal epithelium; deeper layers of the stroma and endothelium are typically unaffected. (Injury thresholds for keratocytes and corneal endothelium will be discussed later in this chapter.) Threshold injury to the epithelium is usually repaired within 24 to 48 hours of exposure and causes no lasting effects.^{6,9-11} The injury first appears as a superficial gray-white spot that is barely visible in the slit-lamp microscope.^{9,12} This damage develops immediately after exposure, although some investigators have applied the criterion of its

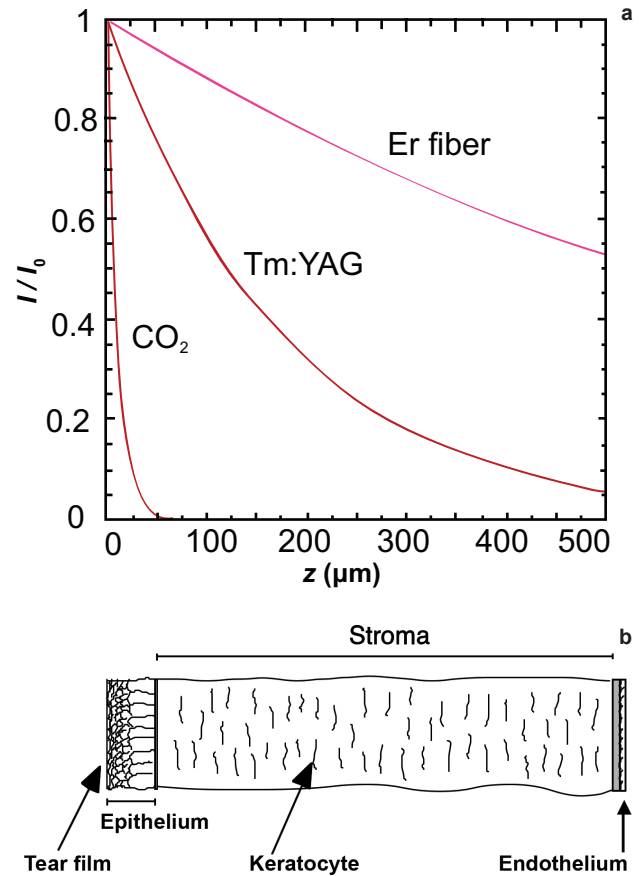


Figure 13-2. (a) Absorption of infrared radiation in cornea as described by Beer's law for wavelengths of 1.54 μ m, 2.02 μ m, and 10.6 μ m. (b) A schematic of the cornea on the same scale. Reproduced with permission from: McCally RL, Bargeron CB, Bonney-Ray JA, Green WR. Laser eye safety research at APL. *Johns Hopkins APL Tech Digest*. 2005;26:48. © The Johns Hopkins University Applied Physics Laboratory.

appearance within 10 minutes,¹¹ 30 minutes,¹²⁻¹⁶ or 60 minutes following exposure.^{17,18} In general, if a minimal lesion has not appeared within this initial period of time, none will develop in the subsequent 24 to 48 hours.^{6,11} (However, one study found the contrary: Ham and Mueller reported the development of corneal lesions 24 hours following 100-second exposures to 1.55 μ m radiation at very low irradiance levels.¹⁹ This puzzling result will be discussed in more detail later in this chapter.)

Threshold exposure levels are determined by delivering a series of exposures with fixed irradiance and varying exposure durations, or with fixed exposure duration and varying irradiance levels. Observations can then be made to determine which exposures produce a lesion and which do not. Many investigators have used the probit method to ana-

lyze such data^{10,12,14,17,20}; this method assumes that a dose-response function will describe the probability that an exposure will produce a lesion.^{21,22} The probit analysis can thus be used to determine ED₅₀, which is that dose for which there exists a 50% probability of injury in the form of a visible lesion. A bracketing procedure is used to broadly bracket exposures above and below threshold. The bracket is then narrowed until only about a 10% difference remains in either the irradiance or radiant exposure for exposures that produce minimal lesions and those that produce none. The threshold is taken to be at the center of the bracket.^{11,13,15,16,23} Some experiments of this type have yielded very well-defined

thresholds involving little or no overlap between exposures that produce minimal lesions and those that do not.

Animal Models

Many investigations of corneal injury thresholds have used New Zealand white or Dutch belted rabbits.^{6,11,13-16,19,23-25} Rhesus and owl monkeys also have been used.^{9,12,14,17,18} One purpose of the latter studies was to determine if damage thresholds differ between species. No such difference has been found, thus increasing confidence that thresholds measured in animal subjects likely also apply to human subjects.¹⁴

CORNEAL INJURY THRESHOLDS AND PERMISSIBLE EXPOSURE LIMITS FOR CARBON DIOXIDE LASERS

Most laser biological threshold studies have focused on understanding biological thresholds and thermal injury mechanisms at the ubiquitous CO₂ laser wavelength of 10.6 μm . As explained above, radiation at this wavelength is strongly absorbed at a depth of just ~ 10 μm . Thus, CO₂ radiation would be almost entirely absorbed within the corneal epithelium. Limited studies of corneal injury thresholds have also been done using a hydrogen fluoride laser at wavelengths of 2.7 and 2.8 μm , with corresponding absorption depths of 16 and 2 μm , and a deuterium-fluoride laser at a wavelength of 3.73 μm with an absorption depth of 76 μm .

Wavelengths in the mid-infrared spectral region between 1.3 and 3 μm do not penetrate to the retina, but overexposure to these wavelengths can, in fact, cause painful and visually disabling corneal injuries. Moreover, optical aids such as binoculars and telescopes readily transmit these spectral wavelengths and greatly increase corneal irradiance at the eyepiece. For example, a 10 \times sighting telescope would increase corneal irradiance by more than 50-fold. Thus, irradiances that may be relatively "safe" to the unaided eye can be amplified to very dangerous levels by optical aids.

With the large number of fire-control telescopes and binoculars now on the battlefield, service members can be exposed to dangerous infrared wavelengths from anti-sensor lasers. Depending on the magnifying power and entrance aperture of telescopic optics, the cornea could be exposed to a range of laser spot sizes. Certain laser wavelengths, particularly those in the 1.4 to 1.7 μm range, are much more likely to damage the corneal endothelium, and thus are more likely to involve delayed effects and corneal healing.

Before about 1990, only a few studies had been done on corneal injury thresholds at laser wavelengths in the mid-infrared spectrum. Stuck et al¹⁷ investigated

thresholds for short pulses of holmium laser radiation at 2.06 μm (absorption depth ~ 250 μm) and Er glass laser radiation at 1.54 μm (absorption depth $> 1,000$ μm). Other studies of Er glass radiation using Q-switched pulses were performed by Lund et al¹⁸ and Avdeev et al.²⁶ Ham and Mueller also reported damage thresholds for continuous wave exposures from a laser diode operating at 1.54 μm .^{19,27}

Since 1990, there have been several extensive investigations at penetrating wavelengths. McCally et al¹⁵ and McCally and Barger^{16,28} determined thresholds for single- and multiple-pulse exposures from Tm:YAG laser radiation at 2.02 μm (absorption depth 174 μm). McCally and Barger also determined the diameter dependence of thresholds for single-pulse exposures from Er fiber laser radiation at 1.54 μm .²⁹⁻³¹ Finally, Zuclich et al determined injury thresholds for cornea, lens, and retina from highly penetrating neodymium-doped yttrium aluminum garnet (Nd:YAG) laser radiation at 1.318 and 1.356 μm .^{32,33} The results and implications of these investigations of corneal injury thresholds for infrared radiation are discussed in the following sections.

Epithelial Injury Thresholds

Dependence on Exposure Duration

Many early studies of the ocular effects of CO₂ lasers were concerned primarily with damage from relatively high exposure levels.^{5,6,8,25} Researchers then turned their attention to determining the minimum radiant exposure or irradiance levels that produce minimal (threshold) corneal damage. Because CO₂ radiation is almost entirely absorbed in the corneal epithelium, threshold damage is confined to this cellular layer.

TABLE 13-2

EPITHELIAL DAMAGE THRESHOLDS FOR CARBON DIOXIDE LASER RADIATION (EXPOSURE DURATIONS > 1 MILLISECOND)

τ (s)	H_{th} (J/cm ²)	I_{th} (W/cm ²)	Beam diameter* (cm)	ΔT_{max}^{\dagger} (°C)	Reference
0.00096	0.599	624	0.102	53.9	1
0.001	0.800	800	0.250	NC	2
0.002	0.970	485	0.250	NC	2
0.0035	0.550	157	0.400	NC	3
0.0039	0.690	177	0.180	47.0	1
0.0092	0.793	86.2	0.252	41.4	1
0.010	0.725	72.5	0.250	NC	2
0.010	0.770	77.0	0.400	NC	3
0.015	0.964	64.3	0.178	42.2	1
0.018	0.945	51.1	0.180	38.1	1
0.019	1.092	57.2	0.254	43.6	1
0.031	1.20	38.8	0.260	39.5	1
0.055	1.20	21.8	0.400	NC	3
0.100	2.46	24.6 [‡]	0.250	NC	4
0.101	2.07	20.4	0.158	39.5	1
0.498	4.48	8.99	0.182	37.9	1
0.500	4.69	9.39	0.224	41.0	1
0.977	6.31	6.46	0.244	38.3	1
1.00	7.70	7.70	0.250	NC	2
5.00	15.0	3.00	0.250	NC	2
9.73	28.1	2.89	0.248	34.7	1
900	220	0.244	1.04 [§]	NC	5
1,800	360	0.200	1.04 [§]	NC	5

*Gaussian beam (1/e diameter) unless noted otherwise.

[†]Calculated on the beam axis 10 μ m beneath tear surface.

[‡]Average value of thresholds for Dutch belted rabbit, rhesus monkey, and owl monkey.

[§]Uniform beam distribution.

τ : exposure duration

H_{th} : threshold radiant exposure per pulse

I_{th} : irradiance threshold

ΔT_{max} : maximum temperature increase

NC: not calculated for this exposure condition

(1) Barger CB, Deters OJ, Farrell RA, McCally RL. Epithelial damage in rabbit corneas exposed to CO₂ laser radiation. *Health Phys.* 1989;56:85–95. (2) Beatrice ES, Stuck BE. Ocular effects of laser radiation: Cornea and anterior chamber. In: *NATO-AGARD Publication No. LS-79*. Neuilly sur Seine, France: NATO-AGARD: 1975: 5-1-5-5. (3) Peppers NA, Vassiliadis A, Dedrick LG, et al. Cornea damage thresholds for CO₂ laser radiation. *Appl Opt.* 1969;8:377–381. (4) Byer HH, Carpino E, Stuck BE. *Determination of the Thresholds of CO₂ Laser Corneal Damage to Owl Monkeys, Rhesus Monkeys, and Dutch Belted Rabbits*. Philadelphia, PA: Frankford Arsenal; 1972. Report M72-3-1; DTIC AD9010862. (5) Fine BS, Fine S, Feigen MS, MacKeen D. Corneal injury threshold to carbon dioxide laser radiation. *Am J Ophthalmol.* 1968;1–14.

Information about damage threshold exposures provides a rational basis for setting laser safety standards.

Most threshold determinations have been made using lasers operating in the fundamental transverse

electromagnetic (TEM₀₀) Gaussian mode, which has a Gaussian irradiance profile given by

$$(2) \quad I(r) = I_0 \exp(-r/r_{1/e})^2$$

TABLE 13-3
EPITHELIAL DAMAGE THRESHOLDS FOR
CARBON DIOXIDE LASER RADIATION
(EXPOSURE DURATIONS < 1 MILLISECOND)

τ (ns)	H_{th} (mJ/cm ²)	Beam diameter* (cm)	ΔT_{max}^{\dagger} (°C)	Reference
1.4	6.1 [‡]	0.90 [§]	1.80	1
1.4	14.7 [‡]	0.90 [§]	4.33	1
1.7	660 [¶]	0.424	65.0	2
25.0	1,080 [¶]	0.424	106	2
80.0	307	0.372	30.2	3
120	350	0.320	34.4	4
250	360 [¶]	0.424	35.5	2

*Gaussian beam (1/e diameter) unless noted otherwise.

[†]Calculated on the beam axis 10 μ m beneath tear surface.

[‡]Slight stippling at 48 hours postexposure.

[§]Uniform beam distribution.

[¶]Lowest exposure for which immediate damage was reported.

^{††}Values are twice those reported by Zuclich et al² to correct for the fact that they divided the total incident energy by the 1/e² area to obtain the radiant exposure.

τ : exposure duration

H_{th} : threshold radiant exposure per pulse

ΔT_{max} : maximum temperature increase

(1) Mueller HA, Ham WJ. *The Ocular Effects of Single Pulses of 10.6 μ m and 2.5–3.0 μ m Q-Switched Laser Radiation*. Los Alamos, NM: Los Alamos National Laboratory; 1976. L-Division Report. (2) Zuclich JA, Blankenstein MF, Thomas SJ, Harrison RF. Corneal damage induced by pulsed CO₂ laser radiation. *Health Phys.* 1984;47:829–835. (3) McCally RL, Bargerion CB. Epithelial damage thresholds for multiple-pulse exposures to 80 ns pulses of CO₂ laser radiation. *Health Phys.* 2001;80:41–46. (4) Lee ST, Anderson T, Zhang H, Flotte TJ, Doukas AG. Alteration of cell membrane by stress waves in-vitro. *Ultrasound Med Biol.* 1996;22:1285–1293.

Here the peak irradiance, I_0 , is related to the total laser power, P , by $I_0 = P/A_{1/e}$, where $A_{1/e}$ is the area within the 1/e radius, $r_{1/e}$. Note that some investigators have used the 1/e² radius to characterize the beam. In this case, $I_0 = 2P/A_{1/e}^2$, where $A_{1/e}^2$ is the area within the 1/e² radius. Obviously, a similar relationship holds for radiant exposure. Use of either the fundamental TEM₀₀ mode or a beam with a uniform irradiance profile (see Fine et al²⁴) allows for easy comparisons between experimental results. Moreover, as will be discussed later in this chapter, use of such beam profiles facilitates comparisons with thermal models.

Epithelial injury thresholds for single pulses of CO₂ radiation have been determined for exposure durations ranging from nanoseconds to 30 minutes. Table 13-2 lists the available threshold data for CO₂

exposures from ~1 ms to 30 minutes, and Table 13-3 lists thresholds for exposures from 1.4 to 250 ns. These threshold radiant exposures and irradiances are the peak values (see Equation 2). Also listed are the calculated peak temperature increases that would result in each case. These will be discussed in the section on thermal models later in this chapter. Excepting the 1.4-ns exposures used by Mueller and Ham (see Table 13-3)³⁴ and the very long exposures investigated by Fine et al (see Table 13-2),²⁴ which were done using a uniform beam profile, all other exposures were done with Gaussian beam profile lasers. Data for exposure durations shorter than 10 seconds are plotted in Figure 13-3. The following section will begin with discussion of threshold data for exposures with durations greater than or equal to 1 ms, and then consider thresholds for shorter duration exposures.

Although the various investigators found some minor differences in the thresholds obtained for exposure durations over 1 ms—especially for durations between 1 and 4 ms—there is remarkable agreement overall. There are several possible reasons for the minor differences observed, including different laser beam diameters, the use of anesthetized versus non-anesthetized animals, different types of anesthesia, variability in tear film thickness, different threshold determination methods, and possible experimental dosimetry errors. Threshold dependency on laser beam diameter will be discussed later in this chapter, but for present purposes, it should simply be noted that for exposure durations greater than ~0.2 second, thresholds are sensitive to beam diameter for diameters less than 0.3 cm.

In the investigations performed by Bargerion et al,¹³ Beatrice and Stuck,³⁵ and Byer et al,¹⁴ experimental animals were anesthetized. In the studies conducted by Peppers et al²⁰ and Fine et al,²⁴ experimental animals were not anesthetized. Bargerion et al used a mixture of ketamine hydrochloride and xylazine as well as topical proparacaine hydrochloride,¹³ whereas Beatrice and Stuck³⁵ used either sodium pentobarbital or halothane gas (this information was inferred from the paper by Brownell and Stuck,¹² which discussed these experiments). Byer et al used sodium pentobarbital.¹⁴ Because the absorption depth of CO₂ radiation is only ~10 μ m, threshold exposures are extremely sensitive to tear film thickness. The thickness of normal tear film is about 7 μ m.¹ If irrigation is not carefully controlled, absorption differences in the resulting thicker or thinner tear layer can be substantial and may exert a significant influence on resulting temperature increase in the epithelium. Finally, Bargerion et al applied a bracketing procedure to determine thresholds, whereas the other investigators used probit methods.

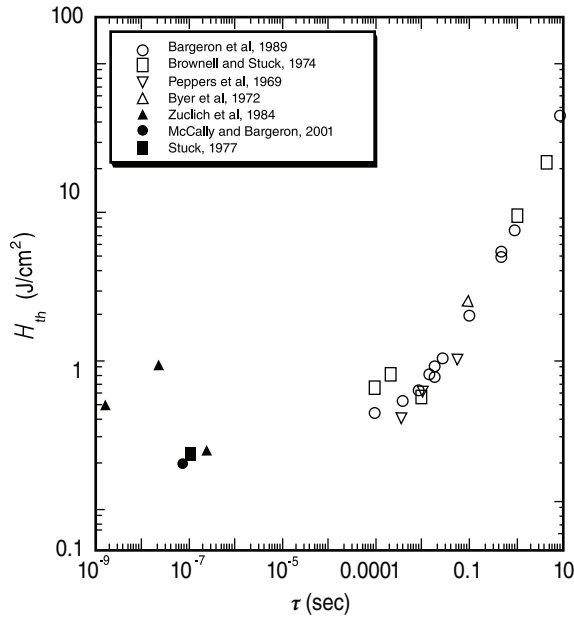


Figure 13-3. Epithelial injury threshold radiant exposures for single pulses of carbon dioxide (CO_2) laser radiation as a function of exposure duration.

H_{th} : radiant exposure per pulse; τ : duration

Data sources: (1) Bargeron CB, Deters OJ, Farrell RA, McCally RL. Epithelial damage in rabbit corneas exposed to CO_2 laser radiation. *Health Phys.* 1989;56:85–95. (2) Brownell AS, Stuck BE. Ocular and skin hazards from CO_2 laser radiation. In: *Proceedings of the 1974 Army Science Conference, US Military Academy, West Point, NY, June 18–21, 1974, Vol 1*. Washington, DC: Office of the Chief of Research and Development, Department of the Army; 1974;1: 123–137. DTIC AD0785609. (3) Peppers NA, Vassiliadis A, Dedrick LG, et al. Cornea damage thresholds for CO_2 laser radiation. *Appl Opt.* 1969;8:377–381. (4) Byer HH, Carpino E, Stuck BE. *Determination of the Thresholds of CO_2 Laser Corneal Damage to Owl Monkeys, Rhesus Monkeys, and Dutch Belted Rabbits*. Philadelphia, PA: Frankford Arsenal; 1972. Report M72-3-1; DTIC AD9010862. (5) Zuclich JA, Blankenstein MF, Thomas SJ, Harrison RF. Corneal damage induced by pulsed CO_2 laser radiation. *Health Phys.* 1984;47:829–835. (6) McCally RL, Bargeron CB. Epithelial damage thresholds for multiple-pulse exposures to 80 ns pulses of CO_2 laser radiation. *Health Phys.* 2001;80:41–46.

In a lesion produced by an exposure slightly above the damage threshold, there was a central area of epithelial edema that extended through all cell layers.³¹ Within this area the cells were moderately disrupted, with edematous spaces between the cells as well. This is typical of thermal lesions. Indeed, damage for exposure durations over 1 ms is thermal, and thresholds can be correlated either by a modified critical temperature model or by a damage integral model (these models and their predictions are discussed later in this chapter).^{12,13,20,36}

There are fewer data points for exposure durations shorter than 1 ms (see Table 13-3), and more variability occurs among these data than is seen for longer-duration exposures. In particular, the thresholds at 1.4 ns and 1.7 ns differ by nearly two orders of magnitude. Unlike other thresholds, damage from the lowest threshold reported by Ham and Mueller had a latency period of 48 hours, but even the exposure that produced immediate damage was 45 times lower than the (similar) 1.7-ns threshold obtained by Zuclich et al.^{37,38} Other differences between experiments were considered unlikely causes of the discrepancy. Zuclich et al attributed threshold damage for their exposures (1.7 ns to 250 ns) to a thermal mechanism, whereas Ham and Mueller attributed damage to mechanical rupture or stress caused by sonic transients.^{11,34,37,38} Both groups reported hearing an audible report from the cornea at exposure levels that produced lesions. Thus, acoustic damage mechanisms should be considered.

Some studies found that large temperature gradients at the anterior surface of the cornea may produce pressure transients via a thermoelastic process.^{39–43} Indeed, Farrell et al⁴¹ presented histology of near-threshold lesions resulting from 80-ns pulses that had features consistent with tensile stress and thermal damage; resulting disruptions of the superficial epithelial cells were consistent with the type of structural alteration that might be produced by a tensile stress wave. In this regard, it is noteworthy that the thermoelastic stress wave generated by laser absorption at free surfaces consisted of a compression wave followed by a tensile wave.^{40,42,43} However, vacuolation and loss of well-defined organelles in the anterior epithelial cells are characteristic of thermal damage.

The temperature increases calculated as those that would result from thresholds obtained by Mueller and Ham are too low (see Table 13-3) to be consistent with any known thermal mechanism.^{34,41} However, temperature increases that would result from the 1.7-ns and 25-ns thresholds obtained by Zuclich et al are in reasonable agreement with the empirical modified critical temperature model originally proposed by Egbert and Maher.³⁶ According to this model, threshold damage occurs when the tissue reaches a critical damage temperature, which is a weak function of exposure duration. To produce damage, short pulses should require greater temperature increases than do longer pulses. Thus, the thresholds for 80-ns,²³ 120-ns, and 250-ns¹¹ pulses are not in good agreement with the empirical modified critical temperature model. Nevertheless, McCally and Bargeron²³ showed that threshold damage from 80-ns pulses involves a substantial thermal component. Because stress waves can decrease cell viability and increase permeability,^{43,44} McCally and

Bargeron suggested that although thermoelastic stress waves may not be the primary mechanism of damage, they may serve to potentiate thermal damage and thus cause damage to occur at a lower temperature.

Dependence on Beam Diameter

If the modified critical temperature damage model provides a valid description of threshold epithelial damage, damage thresholds should have the same dependence on beam diameter.^{7,13} For laser beams that have a Gaussian irradiance profile (see Equation 2), theory predicts that the irradiance (or radiant exposure) required to produce a given temperature rise depends on the diameter of the laser beam. This dependence is due to radial heat conduction. Exposures from small-diameter beams produce larger temperature gradients in the radial direction than do exposures from large-diameter beams. Consequently, more heat is conducted away in the radial direction from small-diameter beams, and larger irradiances are required to produce a given temperature increase on the beam axis.

Damage threshold dependence on beam diameter has been tested experimentally.^{7,13} As predicted by the modified critical temperature damage model, the irradiance required to produce threshold damage indeed increases as the beam diameter decreases. Furthermore, as expected from theory, the threshold dependence beam diameter also depends on exposure

duration. The effect of beam diameter on threshold irradiance manifests itself at increasingly large beam diameters as exposure duration is increased.

Repetitive Pulse Exposures

Many laser systems emit sequences of pulses. Although there have been several studies of retinal damage from such systems,^{18,45-47} Farrell et al⁷ and Bargeron et al¹³ were the first to study threshold corneal damage from sequences of subthreshold pulses. As these investigators observed, it is a more complex task to specify exposure conditions for pulse sequences than to describe single pulse exposures. In addition to peak irradiance (or peak radiant exposure), 1/e beam radius, and pulse duration, it is also necessary to specify the number of pulses (*N*) and pulse repetition frequency (PRF).^{7,13} In one set of experiments, irradiance and beam diameter were held (approximately) constant and individual pulse duration was varied to determine the threshold for several values of *N* and two values of PRF. The results of these experiments are listed in Table 13-4.^{7,13} In subsequent experiments, pulse durations and beam radius were held (approximately) constant and the radiant exposure per pulse was varied to determine the thresholds for a variety of values of *N* and PRF. Table 13-5 lists results for exposures with individual pulse durations of ~10 ms and ~1 ms,^{7,13} and Table 13-6 lists results for exposures with individual pulse durations of 80 ns.²³ Included in these

**TABLE 13-4
MULTIPLE-PULSE INJURY THRESHOLDS**

PRF (Hz)	<i>N</i>	<i>I</i> _{th} [*] (W/cm ²)	τ (s)	<i>H</i> _{th} [*] (J/cm ² /pulse)	Beam diameter [†] (cm)	ΔT_{max} [‡] (°C)
1	1	9.39	0.500	4.69	0.224	41.0
1	2	9.82	0.370	3.63	0.222	44.6
1	4	9.73	0.270	2.63	0.220	42.3
1	8	11.2	0.240	2.69	0.206	48.3
10	8	10.6	0.080	0.848	0.210	47.3

*Threshold irradiances and radiant exposures are peak values.
[†]Gaussian beam (1/e diameter).
[‡]Calculated on the beam axis 10 μm beneath the anterior tear surface.
 PRF: pulse repetition frequency
 τ : duration
*H*_{th}: threshold radiant exposure per pulse
*I*_{th}: irradiance threshold
 ΔT_{max} : maximum temperature increase
 Adapted with permission from: Farrell RA, McCally RL, Bargeron CB, Green WR. *Structural Alterations in the Cornea From Exposure to Infrared Radiation*. Laurel, MD: Applied Physics Laboratory, Johns Hopkins University; 1985: 31. Report TG 1364.

TABLE 13-5
MULTIPLE-PULSE INJURY THRESHOLDS FOR ~10- AND ~1-MILLISECOND PULSES

PRF (Hz)	N	τ (s $\times 10^{-3}$)	I_{th}^* (W/cm ²)	H_{th}^* (J/cm ² /pulse)	Beam diameter [†] (cm)	$\Delta T_{max}^{\ddagger}$ (°C)
1	1 [‡]	9.2	86.2	0.79	0.252	41.4
1	4	10.1	79.6	0.804	0.172	43.4
1	32	9.3	66.8	0.621	0.250	38.4
10	4	9.7	60.0	0.582	0.256	43.3
10	32	10.9	32.7	0.356	0.244	44.6
10	128	9.2	25.3	0.233	0.270	39.8
20	4	10.0	55.3	0.553	0.252	46.8
20	32	9.9	27.8	0.275	0.240	47.7
20	128	8.9	16.4	0.146	0.276	38.8
1	1 [§]	0.96	624	0.599	0.102	53.9
20	10	0.94	239	0.225	0.186	34.7
20	100	0.95	171	0.162	0.174	39.0
20	500	0.92	122	0.112	0.190	33.0
100	10	0.96	153	0.147	0.202	36.0
100	100	0.95	59.6	0.057	0.196	35.2
100	999	0.96	42.0	0.040	0.174	40.1

*Threshold irradiances and radiant exposures are peak values.

[†]Gaussian beam (1/e diameter).

[‡]Calculated on the beam axis 10 μ m beneath the anterior tear surface.

[§]Data are from Table 13-2.

τ : exposure duration

H_{th} : threshold radiant exposure per pulse

I_{th} : irradiance threshold

PRF: pulse repetition frequency

ΔT_{max} : maximum temperature increase

Adapted with permission from: Farrell RA, McCally RL, Bargeron CB, Green WR. *Structural Alterations in the Cornea From Exposure to Infrared Radiation*. Laurel, MD: Applied Physics Laboratory, Johns Hopkins University; 1985: 33. Report TG 1364.

three tables are the maximum temperatures attained at the conclusion of the respective pulse sequences. Temperatures were calculated on the beam axis, 10 μ m beneath the tear surface. Figure 13-4 shows results of these temperature calculations for three of the conditions in Table 13-5.

Figure 13-4 shows wide variability among the temperature histories for the different exposures. Owing to the complexity of the temperature histories, it is more difficult to deduce a general injury correlation for sequenced pulses than for single-pulse exposure conditions, in which temperatures increase monotonically during exposure. Bargeron et al¹³ calculated the damage integral using parameters appropriate for cornea¹² (see discussion on damage models later in this chapter) for the threshold conditions listed in Table

13-4, and found that it varied by a factor of about 40 for the different conditions. They noted that this variability was substantially greater than has been found in other systems, including single-pulse exposures in cornea,^{12,36,48,49} and concluded that the damage integral model is inappropriate for multiple-pulse exposures in cornea. For exposures having individual pulse widths greater than ~10 ms, peak temperature increases for the exposures in Tables 13-4 and 13-5 average $41.3 \pm 4.7^\circ\text{C}$ (mean \pm standard deviation). Thus, they are constant to within about $\pm 11\%$. Bargeron et al noted that there was some systematic max temperature variation with individual pulse widths. In particular, for pulse widths near 1 ms, $\Delta T_{max} = 36.5 \pm 3.6^\circ\text{C}$, for pulse widths near 10 ms, $\Delta T_{max} = 43 \pm 4.7^\circ\text{C}$, and for pulse widths near 300 ms (from Table 13-3), $\Delta T_{max} =$

TABLE 13-6
MULTIPLE-PULSE INJURY THRESHOLDS FOR
80-NANOSECOND PULSES

PRF (Hz)	N	H_{th}^* (J/cm ² /pulse)	Beam diameter [†] (cm)	$\Delta T_{max}^{\ddagger}$ (°C)
–	1	307	0.372	30.2
10	2	235	0.348	25.7
10	8	228	0.380	32.0
10	32	154	0.378	29.2
10	128	136	0.341	32.4
10	1,024	95	0.321	26.6
16	2	265	0.362	29.7
16	8	205	0.375	31.3
16	32	150	0.373	32.9
16	128	105	0.382	32.8
16	1,024	85	0.358	35.1

*Peak radiant exposure.
[†]Gaussian beam (1/e diameter).
[‡]Calculated on the beam axis 10 μm beneath the anterior tear layer.
 H_{th} : threshold radiant exposure per pulse
 PRF: pulse repetition frequency
 ΔT_{max} : maximum temperature increase
 Adapted with permission from: McCally RL, Barger CB. Epithelial damage thresholds for multiple-pulse exposures to 80 ns pulses of CO₂ laser radiation. *Health Phys.* 2001;80:43.

45.3 ± 3°C, where ± denotes the full range of values.¹³ These ranges are consistent with the experimental uncertainties of ±10%, which arise primarily from the bracketing procedure used to determine thresholds. The authors therefore concluded that injury thresholds for multiple-pulse exposures (with individual pulse widths > ~1 ms) are consistent with a critical temperature damage model.

The calculated maximum temperature increases listed in Table 13-6 for exposures to 80-ns pulse sequences are lower than those for longer individual pulse widths. Nevertheless, they are constant to within ±10% of their mean values, and they are independent of the number of pulses in sequence. For the exposures at 10 Hz, $\Delta T_{max} = 29.4 \pm 2.8^\circ\text{C}$ (mean ± standard deviation), and for the exposures at 16 Hz, $\Delta T_{max} = 32 \pm 2^\circ\text{C}$. These results suggest that the damage mechanism has a substantial thermal component and can be described by a critical temperature damage model.²³ McCally and Barger tested this further by measuring damage thresholds in enucleated eyes that had been cooled to room temperature. They noted that if a critical temperature model is valid, damage should occur

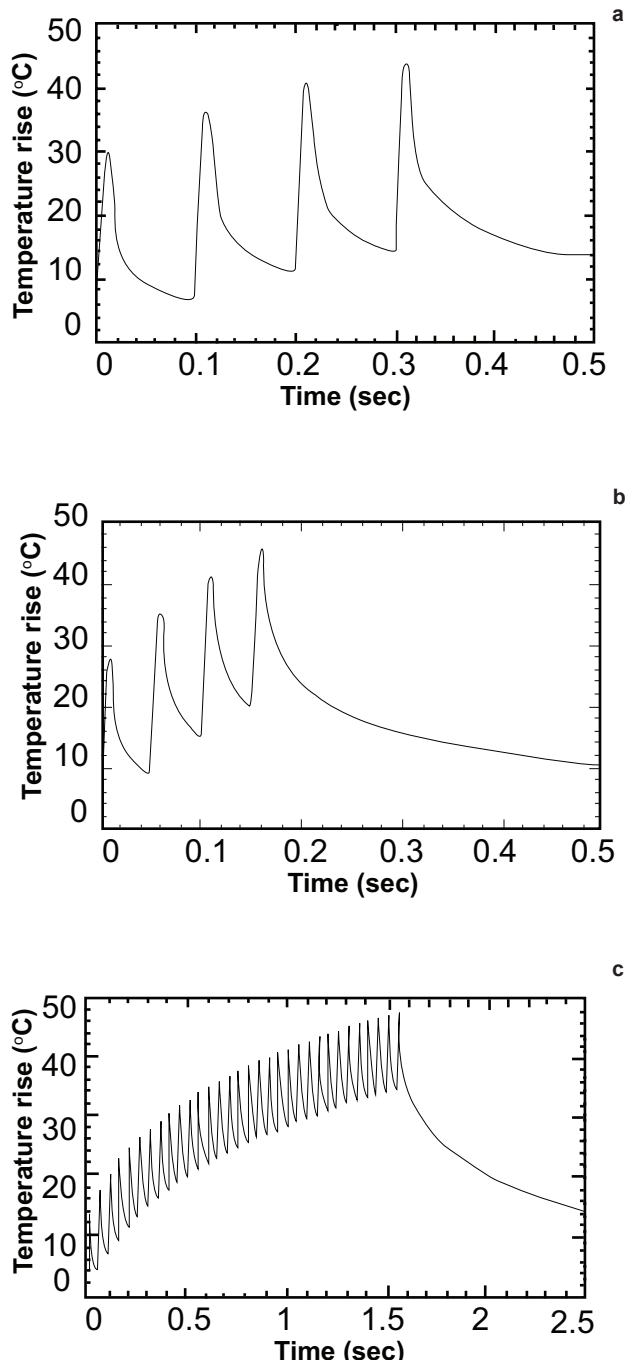


Figure 13-4. Calculated temperature-time histories at a depth of 10 μm below the anterior tear surface for three of the exposures listed in Table 13-5: (a) Four 0.0097 sec pulses at 10 Hz. (b) Four 0.010 sec pulses at 20 Hz. (c) Thirty-two 0.0099 sec pulses at 20 Hz.

Data sources: (1) Farrell RA, McCally RL, Barger CB, Green WR. *Structural Alterations in the Cornea From Exposure to Infrared Radiation*. Laurel, MD: Applied Physics Laboratory, Johns Hopkins University; 1985. Report TG 1364. (2) Barger CB, Deters OJ, Farrell RA, McCally RL. Epithelial damage in rabbit corneas exposed to CO₂ laser radiation. *Health Phys.* 1989;56:85–95.

at the same final critical temperature (not temperature increase).²³ For a cooled cornea, sufficient energy would have to be supplied to raise the temperature, first to the in vivo temperature (assumed to be 35°C⁵⁰) and then to the damage temperature. They tested this hypothesis by measuring thresholds in corneas cooled to 21°C for exposures to sequences of 8 and 32 pulses at 16 Hz. Their results confirmed that the energy needed to produce threshold damage raised the temperature to a level greater than that associated with damage in the in vivo corneas. This result provides additional strong evidence that the damage from sequences of 80-ns pulses has a substantial thermal component. As noted previously with regard to thresholds for single-pulse exposures, McCally and Bargeron suggested that the lower damage temperatures for the 80-ns pulses might be a result of thermal damage potentiated by thermoelastic stress waves.²³

Early investigations of retinal damage from multiple-pulse exposures^{45,51} showed that thresholds were correlated by an empirical relationship of the form

$$(3) \quad H_{th} = CN^{-1/4}$$

In this equation, H_{th} is the radiant exposure per pulse and N is the number of pulses. Ideally, the constant C would be the threshold radiant exposure for a single pulse, and would therefore depend on pulse duration. Bargeron et al¹³ found that their data (see Table 13-5) were consistent with this type of relationship. This question can be considered in more detail, specifically, whether multiple-pulse thresholds can be described by an empirical power law of the form

$$(4) \quad H_{th} = CN^{-\alpha}$$

where the exponent α may differ from 0.25. Figure 13-5 shows threshold radiant exposure per pulse as a function of the number of pulses for exposures with individual pulse widths of ~10 ms and ~1 ms, respectively. The lines are least-squares fits to Equation 4 for $N > 1$. The plots show that Equation 4 indeed describes multiple-pulse threshold data, but that the exponent α appears to increase with pulse repetition frequency. For pulse widths near 10 ms, the values of C are somewhat above the 10-ms single-pulse threshold (21% in the worst case); however, for pulse widths near 1 ms, the values of C are substantially below the 1-ms single-pulse threshold. In the latter case, if the measured single-pulse threshold was used for the constant C , the power law relationship would overestimate thresholds for larger numbers of pulses, and the resultant margin of safety would be reduced. A similar result was reported for multiple-pulse thresholds for 2.02 μm radiation

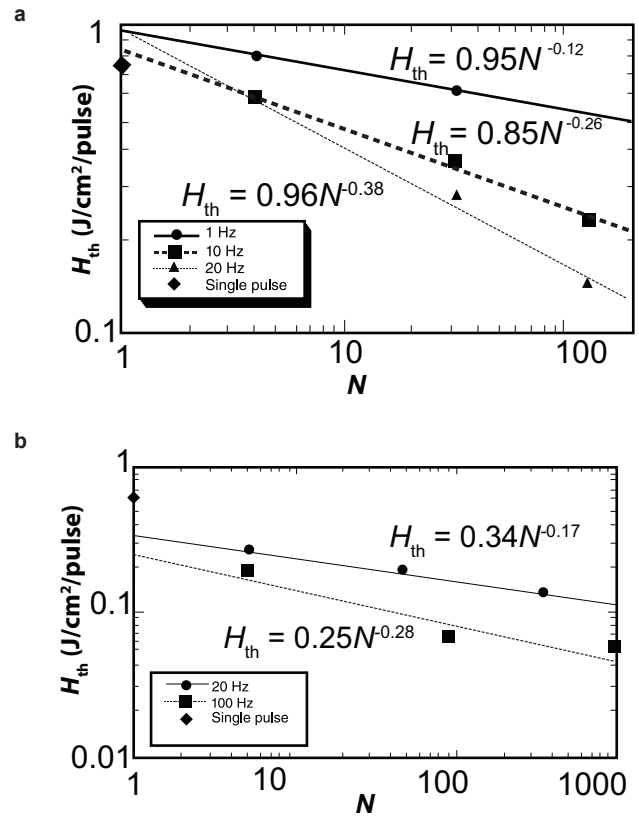


Figure 13-5. The dependence of the threshold radiant exposure per pulse as a function of the number of pulses from a CO₂ laser (data are from Table 13-5). Individual pulse durations are ~10 ms in (a) and ~1 ms in (b). The lines are least-squares fits to a power law of the form $H_{th} = CN^{-\alpha}$. H_{th} : threshold radiant exposure per pulse; C and α : constants that are determined from the fit of the line to the data; N : number of pulses in the repetitive pulse train. Data sources: (1) Farrell RA, McCally RL, Bargeron CB, Green WR. *Structural Alterations in the Cornea From Exposure to Infrared Radiation*. Laurel, MD: Applied Physics Laboratory, Johns Hopkins University; 1985. Report TG 1364. (2) Bargeron CB, Deters OJ, Farrell RA, McCally RL. Epithelial damage in rabbit corneas exposed to CO₂ laser radiation. *Health Phys.* 1989;56:85–95.

from a Tm:YAG laser.¹⁶ These results will be discussed later in this chapter. McCally and Bargeron found that the relationship in Equation 4 accurately described the data in Table 13-6 for sequences of 80-ns pulses.²³ For the 10-Hz thresholds, $C = 0.29 \text{ J/cm}^2/\text{pulse}$ and $\alpha = 0.16$, and for the 16 Hz thresholds, $C = 0.30 \text{ J/cm}^2/\text{pulse}$ and $\alpha = 0.19$. These values of the constant C are very close to the threshold for a single 80-ns pulse ($0.307 \text{ J/cm}^2/\text{pulse}$), and the exponent α again appears to increase with pulse repetition frequency, just as it did for the 1-ms and 10-ms pulses.

Endothelial Injury Thresholds

An early report by Beatrice and Stuck suggested the possibility of endothelial cell damage near the threshold exposure level for epithelial cell injury.³⁵ At exposure levels near the epithelial injury threshold, they reported staining of endothelial cells with the vital stain trypan blue. They noted that such staining is indicative of altered biochemical cell processes and called for further evaluation of the significance of these suggested cellular alterations. Unlike the epithelium, in which threshold lesions are repaired by regenerating cells, the human endothelium is repaired primarily by undamaged cells enlarging and sliding to cover the wound.⁵² Thus, the effect of repeated exposures could be cumulative.

Motivated by the Beatrice and Stuck report, Bargeron et al undertook an investigation to determine endothelial damage thresholds for exposures to CO₂ laser radiation.⁵³ In their experiments, corneas of anesthetized rabbits were exposed to radiation from a CO₂ laser operating in the TEM₀₀ mode, which has a Gaussian irradiance profile given by Equation 2. Thresholds were determined for peak irradiances, I_{0v} of 24.5, 10.0, and 3.6 W/cm², with a beam radius, $r_{1/e} = 0.10$ cm. In determining the damage thresholds, exposure durations were increased above those for the corresponding epithelial injury thresholds at their respective irradiance levels to determine the minimum time to produce endothelial damage. Rabbits were sacrificed 2 hours postexposure, and damage was detected by staining the endothelium with alizarin red S and trypan blue (or indocyanine green).⁵⁴ In a few instances, rabbits receiving the 10 W/cm² exposure were sacrificed at 24 and 48 hours postexposure. The same threshold was obtained.

Table 13-7 lists the exposure times required to produce minimal endothelial damage at the three irradiance levels. These times are approximately five to ten times larger than the epithelial damage thresholds for corresponding irradiances (see Table 13-2). Also listed in Table 13-7 are peak temperature increases on the beam axis at the position of the endothelium (the average thickness of the corneas in the study was 400 μ m). These temperature increases are similar to those found for threshold epithelial damage (see Table 13-2), suggesting that both cell types have a similar critical damage temperature. This result is especially significant with exposures to more penetrating infrared radiation. Such radiation causes much more uniform heating of the entire depth of the cornea; consequently, there is a risk of endothelial damage at exposures close to the epithelial injury threshold. This issue will be discussed in more depth later, relative to 1.54 μ m radiation exposures.

TABLE 13-7

ENDOTHELIAL DAMAGE THRESHOLDS

I_{th}^* (W/cm ²)	τ (s)	Beam diameter [†] (cm)	$\Delta T_{max}^{\ddagger}$ (°C)
24.5	1.0	0.200	50
10.0	5.2	0.200	50
3.6	240	0.200	32

*Peak irradiance.

[†]Gaussian beam (1/e diameter).

[‡]Calculated at depth of 400 μ m, which was the average position of the endothelium in these experiments.

τ : exposure duration

I_{th} : irradiance threshold

ΔT_{max} : maximum temperature increase

Data source: Bargeron CB, Farrell RA, Green WR, McCally RL. Corneal damage from exposure to IR radiation: Rabbit endothelial damage thresholds. *Health Phys.* 1981;40:855-862.

According to Bargeron et al, 2 hours after an exposure at the endothelial damage threshold, a slit-lamp examination showed severe corneal edema at the lesion site and intense stromal light scattering to a depth of $\frac{3}{4}$ to full corneal thickness.⁵³ They noted that the severity of anterior damage depends strongly on irradiance level. In particular, the 1-second, 24.5 W/cm² exposure destroyed the epithelium and severely cratered the stroma. By contrast, the 240-second, 3.5 W/cm² exposure damaged but did not destroy the epithelium and did not cause stromal cratering. Bargeron et al noted further that threshold damage was characterized by distorted cells and uneven staining of cell borders.⁵³ The boundary between damaged and undamaged regions was quite sharp. The staining characteristics of alizarin red S appeared to be more indicative of thermal damage than trypan blue. Trypan blue (or indocyanine green) staining was more sporadic and was often associated with preparation artifacts such as folds.^{53,55}

Corneal Stromal Effects

Keratocyte Injury Thresholds

McCally et al⁵⁵ have observed that when exposed at levels between the epithelial and endothelial damage thresholds, corneas developed characteristic saucer-shaped stromal lesions. At 48 hours postexposure, lesion edges were extremely well defined when viewed in the slit-lamp; histology revealed that the injured area was essentially devoid of cells. Moreover, keratocytes lying just beneath the cell-free region were found to be normal. These observations suggest comparable epithelial and endothelial thresholds. Likewise, stromal

keratocyte injury threshold is sensitive to a comparable laser-induced thermal insult.

To investigate this hypothesis, McCally et al⁵⁵ exposed rabbit corneas at two levels: 9.7 W/cm² (peak irradiance) for 2.5 seconds, and 26 W/cm² for 0.4 seconds. The 1/e beam diameters were 0.188 cm and 0.240 cm, respectively. The durations of these exposures are about four times longer than those required to produce threshold epithelial lesions. The investigators noted that each exposure produced similar damage. One hour after an exposure of 26 W/cm² for 0.4 seconds, there was an interior circular area about 0.2 cm in diameter surrounded by a raised ring of epithelium. Histology revealed that the epithelium was destroyed in the interior circular area. By 48 hours postexposure, such lesions were covered by a smooth layer of epithelial cells and the cornea had recovered its normal thickness.

Slit-lamp photographs were made with geometry that enabled accurate measurements of the depth of the lesion border beneath the corneal surface.⁵⁵ The lesion borders (stromal and epithelial) resulting from the 9.7 W/cm², 2.5-second exposure had a 47°C temperature rise. The lesion borders resulting from the 26 W/cm², 0.4-second exposure had a 52°C temperature rise. These maximum temperature rises, calculated at the center of the beam in the stroma, corresponded closely to those calculated at the edge of the lesion at the epithelial surface. These results suggest that epithelial cells, stromal keratocytes, and endothelial cells have essentially the same thermal damage mechanism.

Healing Response to Deep Stromal Burns

As part of their research supported by what was then the Army Medical Research and Development Command, Farrell et al investigated long-term healing response to deep stromal wounds of the type discussed in the previous section.⁷ In their study, two groups of rabbits were exposed at 25 W/cm² for 0.4 seconds. All exposures were made to the central cornea with a 1/e beam diameter of 0.28 cm. Rabbits in the first group were examined by slit-lamp at 1, 24, and 48 hours, and at 1, 2, 4, and 8 weeks postexposure. Two rabbits were sacrificed at each of these time points, and their corneas were prepared for light and electron microscopy. In the second group, slit-lamp observations were made at 3, 4, and 5 days postexposure, and one rabbit was sacrificed at each of these time points for light and electron micros-

copy. The remaining three rabbits in this group received slit-lamp examinations up to 11 months postexposure.

The characteristics of the wounds at 1 and 48 hours postexposure were described in the previous section. At 24 hours, the completely opaque epithelium remained and covered the wound in some corneas. In other corneas, the opaque covering had sloughed, revealing the bright, light-scattering stromal wound. At this time, a ~30- μ m-thick immature epithelial layer covered the wound. Basal cells had not yet attained their usual columnar form, and there was just a single layer of wing cells.⁷

At 1 week, the appearance of the wound in the slit-lamp resembled its appearance at 48 hours. However, by 2 weeks, the anterior surface of the cornea was slightly flattened and the cornea appeared thinner in the lesion area. Histology revealed that the epithelium was completely normal at 1 week and the stroma was still acellular, although some debris of necrotic keratocytes remained. By 2 weeks postexposure, the stroma was repopulated by keratocytes.⁷

Stromal thinning and flattening persisted at 4 weeks and 8 weeks postexposure. At 4 weeks, the lesion was still clearly visible in a narrow-slit view, but it was only faintly visible in wide-slit views. Stromal scattering was confined to the anterior-most region. At 8 weeks, the anterior scattering was diminished and, although it remained visible in narrow-slit views, the hazy lesion area was very faint in wide-slit views.⁷

No involvement of vascular components (eg, monocytes or polymorphonuclear leukocytes) or vascularization of the cornea was observed during the 8-week period. Moreover, the endothelium and Descemet membrane were observed as normal throughout this period.⁷ It should be noted, however, that the wounds in this study had small diameters compared to the cornea and were located in the central cornea, well away from the limbus. It is possible that a wound of this type could present more serious complications if it were located near the limbus, or if limbal area involvement elicited a vascular response.

Observations of the second series of rabbits were unremarkable at 8 months and 11 months postexposure. By 8 months, the lesion was undetectable using wide-slit illumination, but a very slight increase of anterior scattering was still visible with a narrow slit. The stroma remained thin in the wound area. Lesion appearance was essentially the same at 11 months postexposure.⁷

THERMAL MODELS AND TEMPERATURE MEASUREMENTS

The literature describes several thermal models for calculating the temperature-time history of corneas that have been exposed to laser radiation.^{13,20,36,49,56-58}

These models support calculation of temperatures (or temperature rises) that can be used as inputs to models discussed later in this section. Temperature,

$T(\mathbf{r}, t)$, is obtained from the solution of the heat diffusion equation,

$$(5) \quad \rho C \frac{\partial T(\mathbf{r}, t)}{\partial t} = K \nabla^2 T(\mathbf{r}, t) + A$$

with appropriate boundary conditions.⁵⁹ The absorbing medium (tear layer and cornea) occupies the half-space, $z \geq 0$. In this equation, ρ is the density, C is the heat capacity, ∂ is the partial derivative of temperature T with respect to time t , K is the thermal conductivity, A is the volume production of heat that results from absorption of the incident laser radiation, and the position vector, \mathbf{r} , is usually expressed in cylindrical polar coordinates (r, θ, z). The density, heat capacity, and thermal conductivity of the cornea are assumed to be the same as water.^{13,20,36,48,56-58} The models also assume that there is no scattering and that absorption is described by Beer's law (see Equation 1). In the case of uniform incident illumination as treated by Peppers et al,²⁰ the heat production term is given by

$$(6) \quad A = u(t) \alpha I_0 \exp(-\alpha z)$$

where $u(t)$ describes the time-dependence of the incident radiation, α is the absorption coefficient, and I_0 is the irradiance. In the more general case of an incident Gaussian beam (see Equation 2), the heat production term is given by

$$(7) \quad A = u(t) \alpha I_0 \exp\left(-\alpha z - \frac{r^2}{r_{1/e}^2}\right)$$

where, in this case, I_0 is the peak irradiance.^{56,57} The form of $u(t)$ is usually taken to be that of a Heaviside unit step function, that is, $u(t) = 1$ for $t > 0$ and $u(t) = 0$ for $t \leq 0$.

Mainster et al⁵⁷ provided numerical solutions to Equation 5 for a Gaussian beam incident on the cornea. They ignored convective heat transfer at the cornea-air interface, but did account for the possibility of heat conduction into the air. The initial temperature, $T(\mathbf{r}, 0)$, was assumed to be zero; thus, the solution described the temperature rise. Takata et al⁴⁸ extended this model, and it was also used extensively by Egbert and Maher.³⁶ Peppers et al²⁰ provided an analytic solution to Equation 5 for the case of uniform incident irradiation, again assuming that there was no heat transfer at the cornea-air interface (ie, $\partial T(z, t) / \partial z |_{z=0} = 0$), and also that $T(z, 0) = 0$. Peppers et al noted that the 1-dimensional model would be adequate to predict epithelial temperature increases for short exposures (even with a Gaussian beam), but that it would not be accurate for longer exposures, when the effects of radial heat transfer become important. Subsequently, Chang and Dextrick⁵⁶ developed a Green's function solution to Equation 5 for

an incident Gaussian beam, accounting for radial heat transfer. Their solution assumes the same boundary conditions as those used by Peppers et al. The solution is given by a definite integral

$$(8) \quad T(\mathbf{r}, t) = \frac{1}{2} I_0 k u(t) \int_0^t \exp\left\{-\frac{r^2}{r_{1/e}^2 (1 + 4\kappa\tau/r_{1/e}^2)}\right\} \left[\frac{s(z, \tau)}{1 + 4\kappa\tau/r_{1/e}^2} \right] d\tau$$

where

$$(9) \quad s(z, \tau) = \exp(\alpha^2 \kappa \tau) \left\{ e^{-\alpha z} \operatorname{erfc} \left[\alpha (\kappa \tau)^{1/2} - \frac{z}{2(\kappa \tau)^{1/2}} \right] + e^{\alpha z} \operatorname{erfc} \left[\alpha (\kappa \tau)^{1/2} + \frac{z}{2(\kappa \tau)^{1/2}} \right] \right\}$$

In Equation 9, $\operatorname{erfc}(x)$ is the complementary error function given by

$$\operatorname{erfc}(x) = 1 - \operatorname{erf}(x) = \frac{2}{\sqrt{\pi}} \int_x^\infty e^{-u^2} du$$

Equations 8 and 9 can be integrated numerically to provide the temperature at any position within the cornea.^{13,23,53,55,58,60} Rectangular pulses of duration τ can be represented as the difference of two Heaviside unit step functions. Thus, according to the principle of superposition, the temperature history resulting from exposure to a rectangular pulse of duration τ is given by

$$(10) \quad T_{\text{pulse}}(\mathbf{r}, t) = u(t)T(\mathbf{r}, t) - u(t - \tau)T(\mathbf{r}, t - \tau)$$

Barger et al⁵⁸ conducted a series of experiments to test the efficacy of Chang and Dextrick's model. The epithelial surface of a freshly excised rabbit cornea was irradiated with a CO₂ laser (Gaussian beam profile). The cornea was mounted in a special holder, and its endothelial surface was bathed with Ringer solution pressurized hydrostatically to maintain the natural curvature of the cornea. A 25- μm diameter chromel-alumel thermocouple was inserted through the back of the holder, and its junction was positioned at the endothelial surface with the aid of a slit-lamp microscope. The small thermal inertia associated with this thermocouple gave it a sufficiently rapid response time (conductive heat loss from the junction via the small-diameter wires was negligible). It was essential to align the probe accurately on the axis of the invisible incident Gaussian beam. This was accomplished by moving the entire corneal holder/thermocouple assembly with an x-y micropositioner until a maximum temperature rise was recorded from a very low exposure ($\sim 25 \text{ W/cm}^2$ for 0.05 seconds; this is about half the epithelial damage threshold at this irradiance; see Table 13-3). By this method, Barger et al were able to locate the probe to within about 0.01 cm of the center of the beam ($d_{1/e} = 0.20 \text{ cm}$).

Temperature-time histories were measured with the thermocouple in a 380- μm -thick cornea. The ex-

posures corresponded respectively to the epithelial and endothelial injury thresholds for the given peak irradiance. Temperature was calculated from Chang and Dedrick's model. Although calculated temperatures were higher than measured temperatures, their agreement is quite reasonable. Small discrepancies can be understood in terms of the assumptions of the model and potential sources of error in the measurements. In addition to the assumptions noted above (eg, no heat transfer at the cornea-air interface), the model also ignores effects of water vaporization and collagen melting, as well as the fact that temperature rise at the endothelium can induce convective currents in the fluid bathing the endothelial surface. Because these effects, which would act to reduce the temperature, are not accounted for in the model calculations, the calculated temperature rise would exceed the actual temperature rise. In addition, possible measurement errors (eg, imperfect thermal contact between the probe and endothelial surface, heat loss in thermocouple leads, and finite thermocouple response time), though assumed to be small, also would act to reduce measured temperature. Thus, reasonable agreement between measured and calculated endothelial temperature-time histories indicates that together with the use of thermal properties of water in the calculations, the assumptions of the model are justified, at least for CO₂ radiation. (Barger et al also used a liquid crystal technique to measure the spatial and temporal variations of temperature at the endothelial surface.⁵⁸ Although it is not discussed here, that method led to similar reasonable agreement with the calculations, both on- and off-axis.)

There are two classes of thermal models generally used to predict threshold corneal damage: damage integral models^{12,36,48} and critical temperature (or critical peak temperature) models.^{13,15,16,20,36,53,55,57} A third model has also been proposed¹³ based on the occurrence of an endothermic phase transition at the anterior surface. All three models require temperature calculations such as those discussed in the preceding section.

The damage integral model formulation is based on the idea that thermal damage is due to heat denaturation of constituent tissue molecules (eg, proteins).^{12,61} Damage models usually assume that denaturation can be described by a first-order reaction. The reaction rate is then given by

$$(11) \quad k' = \frac{kT}{h} k^*$$

where k is Boltzmann's constant, T is the absolute temperature, h is Planck's constant, and k^* is the equilibrium constant between the normal and activated states of the molecules undergoing the reaction. The

equilibrium constant is related to the free energy, $\Delta G = \Delta H - T\Delta S$, by

$$(12) \quad k^* = \exp\left(-\frac{\Delta G}{RT}\right) = \exp\left(\frac{\Delta S}{R}\right) \exp\left(-\frac{\Delta H}{RT}\right)$$

where ΔS is the entropy of activation and ΔH is the enthalpy of activation. These relationships are usually expressed in the form of an Arrhenius rate process, $k' = A \exp(-E/RT)$, where the frequency factor, A , is given by

$$A = \frac{kT}{h} \exp\left(\frac{\Delta S}{R}\right)$$

where R is the universal molar gas constant and E is an activation energy associated with the reaction.

These concepts are discussed in detail by Dawes.⁶² Henriques used these ideas to characterize burn injuries in skin.⁶³ He formulated a damage integral given by

$$(13) \quad \Omega(\mathbf{r}, z) = A \int_0^{t^{final}} \exp\left(-\frac{E}{RT(\mathbf{r}, z, t)}\right) dt$$

and chose values of A and E such that $\Omega(\mathbf{r}, z) = 1$ corresponded to irreversible damage. The upper limit of the integral is usually taken to be the time at which the tissue returns to its initial temperature. This formulation has been used successfully to predict threshold injuries in the cornea, particularly for single-pulse exposures. However, as noted previously, it does not provide a good estimate of epithelial injury thresholds from multiple-pulse exposures.

Brownell and Stuck determined values of A and E/R by fitting Equation 13 to their experimentally determined epithelial and skin injury thresholds for exposure to CO₂ laser radiation.¹² For cornea, they found $A = 3.13 \times 10^{61} \text{ sec}^{-1}$ and $E/R = 48,400 \text{ K}$, whereas for skin (white pigs) they found $A = 4.21 \times 10^{63} \text{ sec}^{-1}$ and $E/R = 49,000 \text{ K}$. These skin values differ substantially from those found by Henriques ($A = 3.1 \times 10^{98} \text{ sec}^{-1}$ and $E/R = 75,000 \text{ K}$)⁶³ and later by Takata ($A = 4.3 \times 10^{64} \text{ sec}^{-1}$ and $E/R = 50,000 \text{ K}$ for $317 \text{ K} < T < 323 \text{ K}$ and $A = 9.4 \times 10^{104} \text{ sec}^{-1}$ and $E/R = 80,000 \text{ K}$ for $T \geq 323 \text{ K}$).⁴⁸ Such differences are likely due to the exposure of different areas and types of skin and to the definition of damage endpoints. Obviously, because both A and E are very large numbers, model predictions are highly sensitive to chosen values.

The idea that thermal damage occurs at a critical temperature has long been cited in the biological literature.^{20,36,64} Peppers et al noted that their epithelial damage thresholds for CO₂ laser exposure durations between 3.5 ms and 55 ms were associated with a temperature increase of about 35°C.²⁰ Barger et al found that peak temperature rises were essentially

constant for CO₂ laser threshold exposure durations between 0.01 and 1 second, where they averaged 40 ± 2°C. However, there was a slight variation over this entire range. This type of variation, in which the predicted damage temperature increased as the exposure durations decreased, had been noted earlier by Egbert and Maher.³⁶ They analyzed threshold data from several groups and several laser types in terms of critical temperature damage and damage integral models. To account for slight variation in damage temperature, Egbert and Maher proposed an empirical critical peak temperature damage model as

$$(14) \quad CPT_{EM} = 79.6 \tau^{-0.0152} \text{ } ^\circ\text{C}$$

In this equation, the temperature is calculated on the beam axis at a depth of 6 μm beneath the anterior tear surface, τ is the exposure duration, and the critical peak temperature, CPT_{EM} , is the sum of the peak temperature increase and the ambient temperature of the cornea surface (assumed to be 35°C⁵⁰). Barger et al found that their data were described by a similar empirical relationship,

$$(15) \quad CPT_B = 72 \tau^{-0.020} \text{ } ^\circ\text{C}$$

where peak temperatures were calculated on the beam axis at a depth of 10 μm beneath the anterior tear surface. Empirical relationships such as these depend on damage endpoints and the location where the temperature is calculated. Thus, as was noted by Egbert and Maher, the CPT does not represent an actual damage temperature; rather, it is a convenient parameter that relates the peak temperature at a chosen location on the beam axis to the experimental threshold exposure.

Barger et al postulated that threshold damage might be due to the occurrence of an endothermic phase transition in the lipids of proteins in the epithelium.⁶⁰ They based this idea on the observation that the measured threshold radiant exposure appeared to be approaching an asymptotic value as the exposure duration decreased (for durations 0.001–10 seconds; see Figure 13-3). They also noted that because heat losses due to conduction would be minimal, very-short-duration exposures would approximate the behavior

of a thermally isolated epithelium. Moreover, if damage were associated with an endothermic phase transition, a thermally isolated epithelium would sustain damage when it absorbed enough energy to transition its temperature and to supply the latent heat needed to cause the transition. In the case where the epithelium is not thermally isolated (ie, for longer-duration exposures), additional energy would be necessary to compensate through conduction.

To examine this hypothesis, Barger et al developed a simple two-part, one-dimensional model based on a surface absorber. The first part of the model corresponds to the classic problem of a uniform flux of heat, F_0 , incident on a semi-infinite slab.⁵⁹ The surface temperature rises as the square root of time until the transition temperature, T_c , is reached at time t_c (T_c and t_c are parameters to be determined from the data). At times greater than t_c , the surface temperature remains constant (this is analogous to a water-ice mixture that remains at 0°C during melting). For times greater than t_c , the model corresponds to a second classical problem in which a semi-infinite slab has an initial temperature distribution given by the solution to the first part at t_c and its surface is maintained at T_c .⁵⁹ The amount of heat per unit surface area that goes into the transition, Q_c , was calculated as the difference between the incoming flux and the quantity of heat per unit area per unit time conducted into the cornea (Q_c is a parameter to be determined from the data). Because the data were obtained with a Gaussian beam, the flux was chosen such that, in the absence of a phase transition, calculated peak temperature at the end of the exposure would be the same as for the actual Gaussian beam. The model provided excellent fits to the data for $T_c = 33^\circ\text{C}$ and $Q_c = 0.84 \text{ J/cm}^2$. This value of T_c is in the range found for protein denaturation or for phase transitions of certain lipids.^{65–67} Barger et al¹³ noted that if approximately 5% of the epithelial material in the wound area underwent the phase transition, the value of Q_c would correspond to a latent heat of ~80 calories per gram.¹³ They observed that although this value is about three times greater than values reported for proteins and lipids,^{65–67} the result was encouraging given the model's simplicity and assumptions.

CORNEAL EFFECTS AT OTHER LASER WAVELENGTHS

Epithelial Injury Thresholds for Erbium Glass Laser Radiation

Corneal injury thresholds have been determined for 1.54 μm radiation from Er glass lasers operating in either the free oscillation (long pulse) or Q-switched modes.^{17,18,26} When operating in the long-pulse mode,

an Er glass laser emits an envelope of closely spaced short pulses, each having a duration of ~1.5 μs. The total duration of the envelope is ~1 ms. In the Q-switched mode, the Er glass laser emits a single pulse of duration 40 to 50 ns. The beams of the lasers used in the investigations discussed below were approximately Gaussian.

Lund et al¹⁸ determined the damage threshold in owl monkey cornea for Q-switched radiation. The ED₅₀ was 21 J/cm² (Table 13-8). They investigated exposures up to ~70 J/cm² and found that damage was limited to the cornea even at the highest exposures. All exposures greater than 30 J/cm² produced damage; no damage was observed for exposures below 17 J/cm². Lesions just above threshold were characterized by a shallow depression in the epithelial surface with localized epithelial edema. Grayish opacities were evident in the Bowman layer and anterior stroma. The lesions stained mildly with fluorescein. The more severe lesions had a whiter opacification that penetrated to deeper stromal layers, and wrinkling of the Descemet membrane occurred in some cases. The stromal opacification in these lesions was unchanged for up to 3 weeks postexposure. Histology of the fresh lesions revealed coagulation of the epithelium,

Bowman layer, and anterior stroma. Healed lesions showed epithelial proliferation and collagenous scar tissue in the anterior stroma.

Stuck et al¹⁷ used a slightly modified version of the laser used by Lund et al to determine injury thresholds in rhesus monkeys for the long-pulse mode. With this laser, the duration of the envelope was 0.93 ms at the half-power points and 1.6 ms overall. The ED₅₀ was 9.6 J/cm² (see Table 13-8). The diameter of the lesions was dose dependent; higher doses produced larger-diameter lesions. Doses of 15 J/cm² produced strongly light-scattering conical-shaped lesions in the stroma. The lesions produced in the long-pulse mode were visible immediately after exposure and persisted for up to 10 months with little change of appearance in the scar. No lenticular effects were observed.

One monkey was administered nine closely spaced exposures of 15 to 18 J/cm² in one eye. The eye was observed using specular microscopy for 10 months. After 10 months, the monkey was sacrificed, and the endothelium of the exposed cornea was stained with trypan blue and alizarin red dye. Specular microscopy showed essentially no change in the endothelial cell density in the regions immediately adjacent to the wounds (the region immediately under the wounds could not be observed because of the dense scar). Endothelial cell density determined from the stained cornea was substantially reduced from the preexposed value (2,140 ± 190 cells/mm² vs 3,260 ± 180 cells/mm²), and the cells under the wounds were irregular in shape. Histology of these lesions showed disruption and undulation of the Bowman layer, and the keratocytes were enlarged and irregular in shape throughout the entire depth of the cornea.

Avdeev et al²⁶ determined injury thresholds in chinchilla corneas for both Q-switched and long-pulse modes. Their exposure conditions are listed in Table 13-8. Their ED₅₀ value of 4.7 ± 1.2 J/cm² for the Q-switched mode was nearly four times less than that obtained by Lund et al,¹⁸ and their ED₅₀ value of 7.2 ± 0.6 J/cm² for the long-pulse mode also was somewhat less than that obtained by Stuck et al.¹⁷ The reasons for these differences are not readily apparent. It is unlikely that they are due to the species differences. Moreover, the differences in the reported durations of the Q-switched pulses in the two studies (40 ns vs 50 ns) are unlikely to account for the four-fold difference in thresholds.

Epithelial Injury Thresholds for Holmium Laser Radiation

Stuck et al determined corneal injury thresholds in rhesus monkeys for exposures to 2.06 μm radiation from a Holmium laser operating in either free

TABLE 13-8

EPITHELIAL DAMAGE THRESHOLDS FOR ERBIUM GLASS, HOLMIUM, HYDROGEN FLUORIDE, AND DEUTERIUM-FLUORIDE LASERS

Laser	Wave-length (μm)	τ (sec)	Beam diameter (cm)	ED ₅₀ (J/cm ²)	Ref
Er	1.54	0.93 × 10 ⁻³	0.1*	9.6	1
Er	1.54	1.0 × 10 ⁻³	0.1–0.2	7.2	2
Er	1.54	40 × 10 ⁻⁹	0.1–0.2	4.7	2
Er	1.54	50 × 10 ⁻⁹	0.1*	21.0	3
Ho	2.06	42 × 10 ⁻⁹	0.032	5.2	1
Ho	2.06	100 × 10 ⁻⁶	0.18	2.9	1
HF	2.6–2.9	45 × 10 ⁻⁹	0.082	0.156	4
DF	3.6–3.9	100 × 10 ⁻⁹	0.096	0.377	4

*Gaussian beam (1/e diameter).

τ: exposure duration

DF: deuterium-fluoride

Er: erbium glass

HF: hydrogen fluoride

Ho: holmium

Ref: reference

(1) Stuck BE, Lund DJ, Beatrice ES. Ocular effects of holmium (2.06 μm) and erbium (1.54 μm) laser radiation. *Health Phys.* 1981;40:835–846. (2) Avdeev PS, Gudakovskii YP, Muratov VR, Murzin AG, Fromzel VA. Experimental determination of maximum permissible exposure to laser radiation at 1.54 μm wavelength. *Sov J Quantum Elec.* 1978;8:137–139. (3) Lund DJ, Landers MB, Bresnick GJ, Powell JO, Chester JE, Carver C. Ocular hazards of the Q-switched erbium laser. *Invest Ophthalmol.* 1970;9:463–470. (4) Dunskey IL, Egbert DE. *Corneal Damage Thresholds for Hydrogen and Deuterium Fluoride Chemical Lasers.* Brooks Air Force Base, TX: US Air Force School of Aerospace Medicine; 1973. Report SAM-TR-73-51.

oscillation (long-pulse) or Q-switched modes.¹⁷ In long-pulse mode, the beam profile was not Gaussian and was neither uniform nor circular; laser output consisted of a series of pulses in an envelope whose duration at the half-power points was 100 μ s. The envelope decayed to 0 in 260 μ s. In the Q-switched mode, irradiance profile was approximately Gaussian; the laser emitted a single pulse having a duration of 42 ns at the half-power points. The ED₅₀ for the long-pulse mode was 2.9 J/cm², with an effective beam diameter of 0.018 cm, and increased to ~4.1 J/cm² when the effective beam diameter was reduced to 0.011 cm (see Table 13-8). In the Q-switched mode the ED₅₀ was 5 J/cm², with a beam having a 1/e diam-

eter of 0.032 cm (see Table 13-8). The diameter of the lesions was dose dependent, and their depth extended to the anterior 1/8 to 1/4 of the cornea. Long-pulse lesions near ED₅₀ were not visible after 24 hours, but resulted in a mild stromal scar. Lesions produced near ED₅₀ in the Q-switched mode were difficult to see at 1 week postexposure, but lesions resulting from exposures greater than 8 J/cm² produced a stromal scar that remained visible at 8 months. Histology obtained 3 months after a Q-switched exposure of 19 J/cm² showed alterations in the Bowman layer and a scar in the superficial stroma. For exposures that involved the anterior 1/4 of the stroma, scars were observed 10 months postexposure.

SUMMARY

Dose-response relationships for corneal effects of infrared laser exposure have been characterized in animal models. Computational models that calculate temperature-time histories within the cornea have complemented the experimental threshold determinations to assist in development of permissible exposure limits for a wide range of exposure conditions. Accidental or purposeful military exposures from infrared

lasers will not be limited to the cornea, but will also involve exposure or injury to the ocular adnexa and surrounding skin. With the development and deployment of small, high-energy lasers that emit 50 to 100 kW for ship or area defense, the likelihood increases that military personnel will be exposed. Methods to manage the medical consequences of such exposures must be investigated, and new treatment regimes developed.

REFERENCES

1. Mishima S. Some physiological aspects of the precorneal tear film. *Arch Ophthalmol*. 1965;73:233-241.
2. Maurice DM. The cornea and sclera. In: Davson H, ed. *The Eye*. Orlando, FL: Academic Press; 1984: 1-158.
3. Stringer H, Parr J. Shrinkage temperature of eye collagen. *Nature*. 1964;496:1307.
4. Maher EF. *Transmission and Absorption Coefficients for Ocular Media of the Rhesus Monkey*. Brooks Air Force Base, TX: US Air Force School of Aerospace Medicine; 1978. Report SAM-TR-78-32.
5. Fine BS, Fine S, Peacock GR, Geeraets WJ, Klein E. Preliminary observations on ocular effects of high-power, continuous CO₂ laser radiation. *Am J Ophthalmol*. 1967;64:209-222.
6. Leibowitz HM, Peacock GR. Corneal injury produced by carbon dioxide laser radiation. *Arch Ophthalmol*. 1969;81:713-721.
7. Farrell RA, McCally RL, Barger CB, Green WR. *Structural Alterations in the Cornea From Exposure to Infrared Radiation*. Laurel, MD: Applied Physics Laboratory, Johns Hopkins University; 1985. Report TG 1364.
8. Campbell CJ, Rittler MC, Bredfmeier H, Wallace RA. Ocular effects produced by experimental lasers II. Carbon dioxide laser. *Am J Ophthalmol*. 1968;66:604-614.
9. Borland RG, Brennan DJ, Nicholson AN. Threshold levels for damage of the cornea following irradiation by a continuous wave carbon dioxide (10.6 micron) laser. *Nature*. 1971;234:151-152.
10. Peabody RR, Rose H, Peppers NA, Vassiliadis A. Threshold damage from CO₂ lasers. *Arch Ophthalmol*. 1989;82:105-107.
11. Zuclich JA, Blankenstein MF, Thomas SJ, Harrison RF. Corneal damage induced by pulsed CO₂ laser radiation. *Health Phys*. 1984;47:829-835.

12. Brownell AS, Stuck BE. Ocular and skin hazards from CO₂ laser radiation. In: *Proceedings of the 1974 Army Science Conference, US Military Academy, West Point, NY, June 18–21, 1974, Vol 1*. Washington, DC: Office of the Chief of Research and Development, Department of the Army; 1974: 123–137. DTIC AD0785609.
13. Bargerion CB, Deters OJ, Farrell RA, McCally RL. Epithelial damage in rabbit corneas exposed to CO₂ laser radiation. *Health Phys.* 1989;56:85–95.
14. Byer HH, Carpino E, Stuck BE. *Determination of the Thresholds of CO₂ Laser Corneal Damage to Owl Monkeys, Rhesus Monkeys, and Dutch Belted Rabbits*. Philadelphia, PA: Frankford Arsenal; 1972. Report M72-3-1; DTIC AD9010862.
15. McCally RL, Farrell RA, Bargerion CB. Cornea epithelial damage thresholds in rabbits exposed to Tm:YAG laser radiation at 2.02 μm. *Lasers Surg Med.* 1992;12:598–603.
16. McCally RL, Bargerion CB. Corneal epithelial injury thresholds for multiple-pulse exposures to Tm:YAG laser radiation at 2.02 μm. *Health Phys.* 2003;85:420–427.
17. Stuck BE, Lund DJ, Beatrice ES. Ocular effects of holmium (2.06 μm) and erbium (1.54 μm) laser radiation. *Health Phys.* 1981;40:835–846.
18. Lund DJ, Landers MB, Bresnick GJ, Powell JO, Chester JE, Carver C. Ocular hazards of the Q-switched erbium laser. *Invest Ophthalmol.* 1970;9:463–470.
19. Ham WT, Mueller HA. Ocular effects of laser infrared radiation. *J Laser Appl.* 1991;3:19–21.
20. Peppers NA, Vassiliadis A, Dedrick LG, et al. Cornea damage thresholds for CO₂ laser radiation. *Appl Opt.* 1969;8:377–381.
21. Litchfield JT Jr, Wilcoxon F. A simplified method of evaluating dose effects experiments. *J Pharmacol Exp Ther.* 1949;96:99–113.
22. Finney DJ. *Probit Analysis*. Cambridge, UK: Cambridge University Press; 1971.
23. McCally RL, Bargerion CB. Epithelial damage thresholds for multiple-pulse exposures to 80 ns pulses of CO₂ laser radiation. *Health Phys.* 2001;80:41–46.
24. Fine BS, Fine S, Feigen MS, MacKeen D. Corneal injury threshold to carbon dioxide laser radiation. *Am J Ophthalmol.* 1968:1–14.
25. Geeraets WJ, Fine BS, Fine S. Ocular injury from CO₂ laser radiation. *Acta Ophthalmol.* 1969;47:80–91.
26. Avdeev PS, Gudakovskii YP, Muratov VR, Murzin AG, Fromzel VA. Experimental determination of maximum permissible exposure to laser radiation at 1.54 μm wavelength. *Sov J Quantum Elec.* 1978;8:137–139.
27. Ham WJ, Mueller HA. *Ocular Effects of Infrared Laser Radiation*. Richmond, VA: Virginia Commonwealth University; 1989. Report to Bell Telephone Laboratories.
28. McCally RL, Bargerion CB. Corneal damage thresholds for multiple-pulse exposures to 2.02 μm radiation from a Tm:YAG laser. *Proc SPIE.* 2001;4246:97–103.
29. McCally RL, Bonney-Ray J. Corneal epithelial injury thresholds for exposures to 1.54 μm radiation—dependence on beam diameter. In: *Proceedings of the Laser Bioeffects Meeting at Val de Grâce Hospital, 13–14 June 2002*. Paris, France: French Délégation Générale pour l'Armement (DGA) and the Direction Centrale du Service de Santé des Armées (DCSSA); 2002: 16-1–16-12.
30. McCally RL, Bonney-Ray J, Bargerion CB. Corneal injury thresholds for exposures to 1.54 μm radiation. *Proc SPIE.* 2003;4952:107–112.
31. McCally RL, Bonney-Ray J, Bargerion CB. Corneal epithelial injury thresholds for exposures to 1.54 μm radiation—dependence on beam diameter. *Health Phys.* 2004;87(6):615–624.

32. Zuclich JA, Gagliano DA, Cheney F, et al. Ocular effects of penetrating IR wavelengths. *Proc SPIE*. 1995;2391:112–125.
33. Zuclich JA, Lund DJ, Edsall PR, Stuck BE, Hengst G. High-power lasers in the 1.3–1.4 μm wavelength range: Ocular effects and safety standard implications. *Proc SPIE*. 2001;4246:78–88.
34. Mueller HA, Ham WJ. *The Ocular Effects of Single Pulses of 10.6 μm and 2.5–3.0 μm Q-Switched Laser Radiation*. Los Alamos, NM: Los Alamos National Laboratory; 1976. L-Division Report.
35. Beatrice ES, Stuck BE. Ocular effects of laser radiation: Cornea and anterior chamber. In: *NATO-AGARD Publication No. LS-79*. Neuilly sur Seine, France: NATO-AGARD; 1975: 5-1–5-5.
36. Egbert DE, Maher EF. *Corneal Damage Thresholds for Infrared Laser Exposure: Experimental Data, Model Predictions, and Safety Standards*. Brooks Air Force Base, TX: US Air Force School of Aerospace Medicine; 1977. Report SAM-TR-77-29.
37. Zuclich JA, Blankenstein MF. Comments on pulsed CO_2 -laser corneal injury thresholds. *Health Phys*. 1986;50:552.
38. Ham WT, Mueller HA. Pulsed CO_2 -laser corneal injury thresholds. *Health Phys*. 1986;50:551–552.
39. Sigrist MW, Kneubühl FK. Laser generated stress waves in solids. *J Acoust Soc Am*. 1978;64:1652–1663.
40. Berthelot YH, Busch-Vishniac IJ. Laser-induced thermoacoustic radiation. *J Acoust Soc Am*. 1985;78:2074–2082.
41. Farrell RA, Bargerion CB, McCally RL, Green WR. Corneal effects produced by IR laser radiation. *Proc SPIE*. 1990;1207:59–70.
42. Esenaliev RO, Oraevsky AA, Letokov VS, Karabutov AA, Malinsky TV. Studies of acoustical and shock waves in the pulsed laser ablation of biotissue. *Lasers Surg Med*. 1993;13:470–484.
43. Doukas AG, Flotte TJ. Physical characteristics and biological effects of laser-induced stress waves. *Ultrasound Med Biol*. 1996;22:151–164.
44. Lee ST, Anderson T, Zhang H, Flotte TJ, Doukas AG. Alteration of cell membrane by stress waves in-vitro. *Ultrasound Med Biol*. 1996;22:1285–1293.
45. Stuck BE, Lund DJ, Beatrice ES. *Repetitive Pulse Laser Data and Permissible Exposure Limits*. Presidio of San Francisco, CA: Letterman Army Institute of Research; 1978. Institute Report No. 58.
46. Ham WT, Mueller HA, Wolbarsht ML, Sliney DH. Evaluation of retinal exposures from repetitively pulsed and scanning lasers. *Health Phys*. 1988;54:337–344.
47. Sliney DH, Marshall J. Tissue specific damage to the retinal pigment epithelium. *Lasers Light Ophthalmol*. 1992;5:17–28.
48. Takata AN, Goldfinch L, Hinds JK, Kuan LP, Thomapolis N, Weigandt A. *Thermal Models of Laser-Induced Eye Damage*. Chicago, IL: IIT Research Institute; 1974. Report AD-A-017201.
49. Welsh AJ, Polhamus GD. Measurement and prediction of thermal injury in the retina of the rhesus monkey. *IEEE Trans Biomed Eng*. 1984;31:633–643.
50. Rosenbluth RF, Fatt I. Temperature measurements in the eye. *Exp Eye Res*. 1977;25:325–341.
51. Lund DJ, Stuck BE, Beatrice ES. *Biological Research in Support of Project MILES*. Presidio of San Francisco, CA: Letterman Army Institute of Research; 1981. Institute Report 96.
52. Van Horn DL, Hyndiuk RA. Endothelial wound repair in primate cornea. *Exp Eye Res*. 1975;21:113–124.
53. Bargerion CB, Farrell RA, Green WR, McCally RL. Corneal damage from exposure to IR radiation: Rabbit endothelial damage thresholds. *Health Phys*. 1981;40:855–862.

54. Spence DJ, Peyman GA. A new technique for vital staining of the corneal endothelium. *Invest Ophthalmol.* 1976;15:1000–1002.
55. McCally RL, Bargeron CB, Green WR, Farrell RA. Stromal damage in rabbit corneas exposed to CO₂ laser radiation. *Exp Eye Res.* 1983;37:543–550.
56. Chang HC, Dedrick KG. Corneal damage thresholds of CO₂ laser radiation. *Appl Opt.* 1969;8:126–127.
57. Mainster MA, White TJ, Tips JH. Corneal thermal response to the CO₂ laser. *Appl Opt.* 1970;9:665–667.
58. Bargeron CB, McCally RL, Farrell RA. Calculated and measured endothelial temperature histories of excised rabbit corneas exposed to infrared radiation. *Exp Eye Res.* 1981;32:241–250.
59. Carslaw HS, Jaeger JC. *Conduction of Heat in Solids.* Oxford, UK: Clarendon Press; 1959: 1-49.
60. Bargeron CB, Farrell RA, Green WR, McCally RL. Threshold corneal damage from very short pulses of CO₂ laser radiation. *Invest Ophthalmol Vis Sci.* 1989;30 Suppl 3:S217.
61. Welch AJ. The thermal response of laser irradiated tissue. *IEEE J Quantum Elec.* 1984;QE-20:1471–1481.
62. Dawes EA. *Quantitative Problems in Biochemistry.* 3rd ed. Baltimore, MD: Williams and Wilkins; 1965: 101–125.
63. Henriques FC Jr. Studies of thermal injury; the predictability and the significance of thermally induced rate processes leading to irreversible epidermal injury. *Arch Pathol.* 1947;43:489–502.
64. Joly M. *A Physical Chemical Approach to the Denaturation of Proteins.* New York, NY: Academic Press; 1965.
65. Garrett RR, Flory PJ. Evidence for a reversible first-order phase transition in collagen-diluent mixtures. *Nature.* 1956;177:176–177.
66. Tanford C. *The Hydrophobic Effect: Formation of Micelles and Biological Membranes* New York, NY: John Wiley and Sons; 1973.
67. Tanford C. Protein denaturation. In: Anfinsen CB, Anso ML, Edsall JT, Richards FM, eds. *Advances in Protein Chemistry.* New York, NY: Academic Press; 1968.